Review Article | Oncologic Imaging

eISSN 2005-8330
https://doi.org/10.3348/kjr.2023.0840
Korean J Radiol 2024;25(1):86-102

Korean Journal of Radiology
KJR

Imaging Evaluation of Peritoneal Metastasis: Current and Promising Techniques

Chen Fu[1], Bangxing Zhang[2], Tiankang Guo[3,4,5], Junliang Li[1,3,4,5]*

[1]The First School of Clinical Medical, Gansu University of Chinese Medicine, Lanzhou, Gansu, China
[2]School of Clinical Medicine, Ningxia Medical University, Yinchuan, Ningxia, China
[3]Department of General Surgery, Gansu Provincial Hospital, Lanzhou, Gansu, China
[4]Key Laboratory of Molecular Diagnostics and Precision Medicine for Surgical Oncology in Gansu Province, Gansu Provincial Hospital, Gansu, China
[5]NHC Key Laboratory of Diagnosis and Therapy of Gastrointestinal Tumor, Gansu Provincial Hospital, Lanzhou, Gansu, China

Early diagnosis, accurate assessment, and localization of peritoneal metastasis (PM) are essential for the selection of appropriate treatments and surgical guidance. However, available imaging modalities (computed tomography [CT], conventional magnetic resonance imaging [MRI], and 18fluorodeoxyglucose positron emission tomography [PET]/CT) have limitations. The advent of new imaging techniques and novel molecular imaging agents have revealed molecular processes in the tumor microenvironment as an application for the early diagnosis and assessment of PM as well as real-time guided surgical resection, which has changed clinical management. In contrast to clinical imaging, which is purely qualitative and subjective for interpreting macroscopic structures, radiomics and artificial intelligence (AI) capitalize on high-dimensional numerical data from images that may reflect tumor pathophysiology. A predictive model can be used to predict the occurrence, recurrence, and prognosis of PM, thereby avoiding unnecessary exploratory surgeries. This review summarizes the role and status of different imaging techniques, especially new imaging strategies such as spectral photon-counting CT, fibroblast activation protein inhibitor (FAPI) PET/CT, near-infrared fluorescence imaging, and PET/MRI, for early diagnosis, assessment of surgical indications, and recurrence monitoring in patients with PM. The clinical applications, limitations, and solutions for fluorescence imaging, radiomics, and AI are also discussed.

Keywords: Peritoneal neoplasms; Diagnostic imaging; Molecular imaging; Optical imaging; Radiomics; Artificial intelligence; Deep learning; Machine learning

INTRODUCTION

Peritoneal metastases (PM) generally originate from gastrointestinal malignancies or ovarian cancers (OC). Different primary tumors have different incidences and prognoses, with the relative incidence of PM in OC, gastric cancer (GC), and colorectal cancer (CRC) being as high as 60%–75% [1], 20%–45% [2], and 20%–25%, respectively [3]. However, PM has limited treatment options and a poor prognosis owing to late diagnosis and limited response to treatment with systemic chemotherapy [4,5]. Early diagnosis of PM is essential for optimal treatment (e.g., neoadjuvant chemotherapy [6-9] or conversion therapy [10-12]). The use of complete cytoreduction surgery (CRS) in combination with a multidisciplinary strategy for patients with tumor dissemination limited to the peritoneal region can lead to long-term survival or even a cure [13-15]. Indeed, the severity of peritoneal tumors and the integrity of the operation are the two most important prognostic factors for PM curative management [16-19]. The former is usually quantified using the peritoneal cancer index (PCI) [20], while accurate preoperative evaluation of PCI facilitates the selection of patients who could benefit from CRS [21]. Moreover, complete resection should harmonize sufficient tumor-free margins and the protection of vital structures.

Received: June 22, 2023 **Revised:** September 28, 2023
Accepted: October 8, 2023
*The primary affiliation for the corresponding author is Gansu Provincial Hospital, Lanzhou, Gansu, China.
Corresponding author: Junliang Li, MD, PhD, Department of General Surgery, Gansu Provincial Hospital, 204 Donggang West Road, Lanzhou 730030, Gansu, China
• E-mail: lijl2018@lzu.edu.cn

Korean Journal of Radiology
KJR

Existing imaging techniques are inadequate for clinical diagnosis, and new imaging strategies utilize advancements in imaging equipment and new molecular imaging tracers to improve image contrast and penetration depth for diagnosis, evaluation, and real-time intraoperative guidance for resection. Furthermore, images serve as pictures and provide numerical data. Radiomics and artificial intelligence (AI) may provide diverse information regarding tumor phenotypes and microenvironments that cannot be obtained by traditional imaging evaluations. After filtering, the radiomic signatures are transformed into a multivariable model with predictive ability that can be used as an auxiliary clinical decision-making tool for various predictions related to PM.

In this review, we first discuss the strengths and limitations of existing imaging techniques, highlighting the importance of standardized radiology reporting, new imaging strategies for the early diagnosis of PM, and the latest developments in accurately evaluating and guiding PM surgery, and analyzing their limitations. Finally, the workflow, limitations, and solutions for radiomics and AI are discussed.

Traditional Imaging Modalities for Diagnosing PM

The complex peritoneal structure and excessive overlap of radiological signs between normal tissues, benign diseases, and PM limits the ability of traditional imaging methods to diagnose and evaluate PM [22]. Nevertheless, CT remains the imaging technique of choice in current practice for PM diagnosis because of its speed of acquisition and wide availability [23]; although the limited contrast resolution makes it difficult for computed tomography (CT) to identify equidensity lesions with adjacent invaded tissue density, resulting in a sensitivity ranging from 9.1% to 50% for lesions below 1 cm, and only 11% for those below 0.5 cm [24,25]. In addition to size, CT sensitivity to the right subphrenic space, small intestine mesentery, and serosa can be reduced to 22% [25].

Notably, peritoneal diffusion-weighted imaging (DWI) in combination with T1 and T2 weighted magnetic resonance imaging (MRI) images and delayed gadolinium enhancement improves the diagnostic performance of PM. DWI is used for the diagnosis and evaluation of PM as it can accurately detect small lesions (< 0.5 cm) and evaluate important anatomical sites such as the porta hepatis and hepatoduodenal ligament, small intestine and mesentery, bladder, and trigone by highlighting lesions that lack comparative resolution and are unrecognizable on CT as well as equidensity lesions in affected areas [26-28]. DWI also has a higher sensitivity for mucinous lesions than CT and ^{18}F-fluorodeoxyglucose (FDG) positron emission tomography/computed tomography (PET/CT) and can supplement the diagnosis of patients with pseudomyxoma peritonei [29,30]. However, a limitation in diffusion can also be seen in inflammation and ischemia [31,32]. Therefore, close integration of clinical data and familiarity with diffusion-restricted normal structures such as benign lymph nodes, intestinal mucosa, and spleen remain essential for identification.

^{18}F-FDG PET/CT is primarily used to detect extraperitoneal metastases, particularly in distant lymph nodes. It can serve as a supplementary tool to CT and MRI, especially in patients with increased tumor markers and/or unclear or negative morphological imaging findings, and can be used to detect disease recurrence [33-35]. However, in some cases of high background activity and low affinity, the diagnostic performance of ^{18}F-FDG PET/CT for PM has limitations, including physiological factors such as excretion by the kidneys [36] and uptake by the gastrointestinal tract and diaphragm or liver capsule [37], leading to a low tumor background ratio (TBR). Moreover, the uptake of special tissue types is insufficient, including the non-intestinal diffuse type, signet-ring cell carcinoma, mucinous adenocarcinoma, non-solid type, and poorly differentiated adenocarcinoma [38-41].

Promising Imaging Strategies for Diagnosing PM

Spectral Photon-Counting CT

Spectral photon-counting CT (SPCCT) is a revolutionary upgrade to CT and is equipped with a photon-counting sensor that allows the direct conversion of single X-ray photons into electrical signals and divides the electrical pulse generated by each photon into multiple energy windows by setting different thresholds to achieve spectral separation and material decomposition [42,43]. Compared to dual-energy CT, SPCCT has an extremely high spatial resolution and contrast-to-noise ratio (CNR), reduces the radiation dose, and allows for over two types of multiple-contrast imaging [44,45]. Thus, it is a strong iodine contrast (just above the K-edge 33 KeV) despite conventional or even low doses of intravenous contrast media [46]. Conversely, double-contrast agent SPCCT can better characterize small lesions by collecting and reconstructing multiphase scans (virtual

 https://doi.org/10.3348/kjr.2023.0840

non-contrast images, venous phase, and arterial phase) in one run. In a rat model of colon PM, a dual-contrast protocol between the peritoneum and blood vessels proved that SPCCT had a higher sensitivity (69%) and specificity (100%) than conventional CT for small lesions (< 5 mm) [47]. Additionally, optimizing scanning protocols and implementing reconstruction schemes for SPCCT, such as quantum iterative reconstruction, can improve dose efficiency and image quality [48].

Fibroblast Activation Protein Inhibitor PET/CT

The specific and extremely low physiological radiotracer uptake in vital organs greatly improves the diagnostic performance of fibroblast activation protein inhibitor (FAPI) PET/CT, which can detect primary lesions and special sites/small peritoneal metastases in different types of cancers, especially in patients with GC. Comparisons of the diagnostic performance and other characteristics of ^{68}Ga/^{18}F-FAPI PET/CT and traditional imaging modalities are listed in Table 1.

Imaging Principle and Different Isotope-Labeled FAPI Tracers

Cancer-associated fibroblasts (CAFs), which mainly

Table 1. Comparison of CT, MRI, ^{18}F-FDG PET/CT, and ^{68}Ga/^{18}F-FAPI PET/CT for the diagnosis of PM

	MRI (P + DWI + C)	CT (MD + C)	^{18}F-FDG PET/CT	^{68}Ga/^{18}F-FAPI PET/CT
Ease of use	1. Relatively available 2. Expensive and operator-dependent 3. Long scanning time (30–40 min)	1. Widely available and reproducible 2. Relatively inexpensive 3. Short scanning time (4–5 min)	1. Limited availability 2. More expensive than CT or MRI 3. Moderate scanning time (20 min)	1. Limited availability 2. More expensive than CT or MRI 3. Moderate scanning time (20 min)
Average radiation (mSv)	Exposure-free	15.4	12.2	11
Ideal target	Supplementary examination for evaluation of tumors	Preferred techniques for diagnosis and preoperative evaluation	Important tools for confirming extraperitoneal metastasis, increased tumor markers, and/or unclear or negative morphological imaging	Potentially optimize assessment of PCI, but lack of high-level evidence
Strength	1. Superior soft tissue contrast resolution and contrast resolution 2. Evaluation of the mesentery, bowel serosa, perihepatic, and peripancreatic spaces 3. High sensitivity to cystic/mucinous deposits	1. The superior spatial resolution 2. Evaluation of epigastrium	Provide tumor glucose metabolism and anatomical information	1. High TBR, independence from blood glucose level (no fasting), and rapid renal clearance 2. Evaluation of peritoneum, omentum, mesentery 3. 2–3 mm lesions 4. High sensitivity to mucinous deposits
Weakness	Magnetic sensitive artifacts and motion artifacts	1. Lesions less than 1 cm and limited soft tissue contrast 2. Allergic reactions, pregnancy, liver and kidney dysfunction disabled	1. High background activity and low affinity situation 2. Lesions smaller than 5 mm 3. Affected by blood sugar	Non-specific fibrosis due to various causes (including inflammation, radiation, and surgery)

'CT (MD + C)'means 'multi-detector computed tomography and contrast-enhanced imaging' and 'MRI (P + DWI + C)' means 'includes plain scan, diffusion weighted and contrast-enhanced sequences'. MRI plain scan includes T1 weighted and T2 weighted. MRI contrast-enhanced sequences include non-enhanced + gadolinium enhanced fat-suppressed T1 weighted imaging of the pelvis and abdomen. MD represents multi-detector computed tomography.
CT = computed tomography, MRI = magnetic resonance imaging, FDG = fluorodeoxyglucose, PET = positron emission tomography, FAPI = fibroblast-activated protein inhibitors, PM = peritoneal metastasis, DWI = diffusion-weighted imaging, PCI = peritoneal cancer index, TBR = tumor background ratio

https://doi.org/10.3348/kjr.2023.0840

Korean Journal of Radiology
KJR

constitute the tumor stroma and are barely expressed in normal adult tissues, express high levels of fibroblast activation protein (FAP) [49,50], which is associated with a poor prognosis [51]. Therefore, FAP is a potential target for the diagnosis and treatment of various malignant tumors. Recently, quinoline-based FAPI labeled with ^{68}Ga or ^{18}F were developed and validated for the diagnosis of PM [52] because they provide excellent TBR and significantly reduce the imaging duration (owing to rapid excretion from the kidneys) [53]. Although most centers currently use FAPI tracers labeled with ^{68}Ga, the low quantity produced simultaneously and the short half-life of ^{68}Ga limit its widespread use [54]. ^{18}F has advantageous properties over ^{68}Ga, such as a longer half-life (109.8 min) and lower positron energy (higher spatial resolution) [55]. Currently, radioactive agents such as ^{18}F-FAPI-42 and ^{68}Ga-FAPI-04 are used for the clinical diagnosis of PM. Moreover, ^{18}F-FAPI-42 and ^{68}Ga-FAPI-04 exhibited similar uptake rates; however, the former had a longer half-life [56]. Moreover, the targeted portion of the FAPI is connected to the chelator agent DOTA, which allows for the incorporation of different isotopic couplings for imaging or therapeutic purposes (e.g., ^{177}Lu, ^{90}Y, ^{225}Ac, and ^{64}Cu) [57-59].

Application of PET/CT in the Diagnosis of PM Based on FAPI

A high TBR is one of the most important prerequisites for the clear visualization of lesions, which is indispensable for evaluating tumor severity and optimizing treatment plans (Fig. 1) [60,61]. ^{68}Ga/^{18}F-FAPI does not accumulate in the gastrointestinal tract and liver [62,63]. Regardless of its origin, PM has a strong uptake because the process

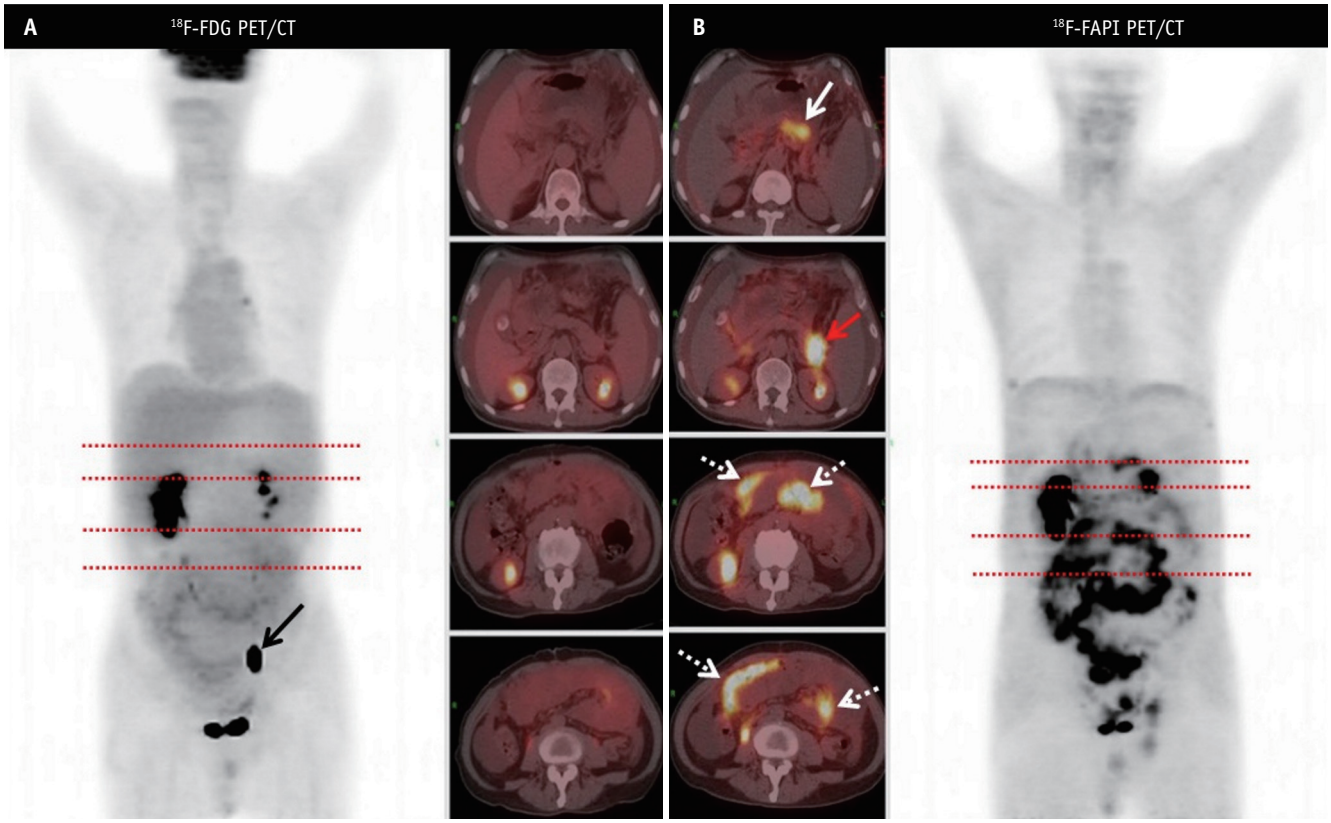

Fig. 1. A 65-year-old male presented with abdominal pain and massive ascites. The cytological examination of the ascites revealed mesothelial cell proliferation. The red dashed lines represent the level of each of the fused axial images. **A:** Images from fluorine 18 (^{18}F) fluorodeoxyglucose (FDG) PET/CT show diffuse radioactive uptake in the mesentery and greater omentum, but ^{18}F-FDG uptake is weak in all the lesions (SUVmax2.82). Intrapelvic hypermetabolic foci is a physiological radioactive accumulation of left ureteral urine (black solid arrow) (left image: anterior maximum intensity projection image from ^{18}F-FDG PET; right images: axial fused PET/CT images). **B:** Images from 18 (^{18}F) fibroblast-activation protein inhibitor (FAPI) PET/CT show intense tracer uptake in the primary lesion of the pancreatic tail (red solid arrow, SUVmax9.55), the lesser curvature of the stomach (white solid arrow, SUVmax4.85) as well as the mesentery and greater omentum (dashed arrows, SUVmax6.46) (right image: anterior maximum intensity projection image from ^{18}F-FAPI PET; left images: axial fused PET/CT images). PET/CT = positron emission tomography/computed tomography, SUV = standard uptake value

https://doi.org/10.3348/kjr.2023.0840

of PM is an intense desmoplastic reaction [64,65]. Güzel et al. [61] found that ^{68}Ga-FAPI-04 PET/CT could show greater lesion extent with higher maximum standardized uptake value (SUVmax) and TBR than ^{18}FDG PET/CT (SUVmax 6.45 vs. 4.1; $P < 0.001$; TBR 14.9 vs. 6.8; $P < 0.001$). There are two types of peritoneal invasion: diffuse and nodular. A high TBR allows for better evaluation of the extent of diffuse small intestine and pelvic involvement as well as complex anatomical sites such as the peripancreas, diffuse liver capsule, or diaphragmatic invasion. Meanwhile, a high TBR can identify very small lesions (2–3 mm), possibly because tumors larger than 2 mm require a support matrix larger than the tumor volume [63,66].

Therefore, ^{68}Ga/^{18}F-FAPI PET/CT can provide a more accurate PCI and has a significantly greater sensitivity than ^{18}F-FDG PET/CT (97.67% vs. 72.09%) and negative predictive value (75% [3/4] vs. 20% [3/15]) [62]. However, the diagnostic performance of these regions remains unclear. Nodular PM showed higher sensitivity (92.74% vs. 39.52%). A previous study indicated that compared with traditional imaging methods (CT, MRI, and ^{18}F-FDG PET/CT), 27.7% (13/47) of patients changed their treatment plans because of the detection of new primary and/or metastatic lesions or clear false-positive lesions on ^{68}Ga FAPI-04 PET/CT [67].

^{68}Ga-FAPI PET/CT is beneficial for individualized therapy of platinum-sensitive recurrent OC. ^{68}Ga-FAPI PET/CT-identified lesions in patients with negative ^{18}F-FDG PET/CT results led to changes in treatment in five patients (5/29, 17.24%) and allowed for R0 resection in 14 (14/29, 48.26%) [68].

Although numerous comparative studies have indicated that FAPI PET/CT is a valuable examination method, its limitations should be noted. First, several studies enrolled small sample sizes (n = 10–60) and exhibited heterogeneity [62,69]. The diagnostic performance of ^{68}Ga/^{18}F-FAPI PET/CT may be exaggerated due to patient distribution bias. For example, more than half of the total sample size included patients with GC, which is sensitive to ^{68}Ga/^{18}F FAPI uptake, whereas ^{18}F-FDG showed low-to-moderate uptake [70]. Second, few studies have compared imaging results with the gold standard for histopathology. Although the sensitivity of FAPI PET/CT compared to other imaging modalities is well established, its cancer specificity and positive predictive value have not been adequately evaluated. Third, some comparative studies did not include patients with benign peritoneal lesions and had a risk of patient selection bias [71]. Moreover, non-specific fibrosis induced by tissue injury, remodeling [72], therapy [63], or inflammation [70] can also increase the uptake of ^{68}Ga-FAPI, resulting in false positives. Currently, the use of FAPI PET/CT is limited to clinical trials. However, numerous studies indicated that FAPI provides a higher TBR than PET. Large-scale comparative studies with long-term follow-ups are still needed to determine the clinical value and superiority of FAPI, as well as to establish a basis for obtaining Food and Drug Administration approval.

Near-Infrared Fluorescence Imaging

It is challenging for surgeons to accurately distinguish between benign and malignant tissues, protect important structures, and discover small lesions deep within the tissue based solely on visual inspection and tactile feedback. In contrast, as an intraoperative decision-making tool, fluorescence imaging objectively guides surgeons to achieve complete CRS or debulking surgery [73] (Fig. 2). Two important factors affecting the performance of fluorescent contrast agents are tumor specificity and penetration depth. The former actively accumulates folate receptor alpha (FRα) and carcinoembryonic antigens (CEAs) in tumor tissue through tumor-specific ligand recognition and has gradually transitioned to clinical trials (Fig. 3). In a phase III clinical trial of OC using OTL38, a near-infrared (NIR) fluorescent probe targeting FRα, additional lesions were not detected by white light, and palpation was detected in 33% of the patients with a sensitivity of 83% [74]. The false positive results may be attributed to the non-specific targeting of lymph nodes (FRβ), but it remains unclear whether the removal of all positive lesions is related to surgical risk, as lymph nodes are potential biomarkers of tumor-activated macrophages associated with epidemic treatment [75,76]. Similarly, SGM-101, an NIR fluorescent probe targeting CEA, is safe and feasible for intraoperative imaging of PM from colorectal and pancreatic ductal adenocarcinomas and can improve surgical outcomes [77,78]. However, one limitation of these probes is that the depth of tissue penetration is insufficient to locate deep lesions. Radionuclides have almost no tissue attenuation and combining them with fluorophores for multimodal imaging may overcome this limitation. In a colorectal PM dose-increasing experiment, 10 mg labetuzumab (an anti-CEA antibody) was jointly marked by 111In and IRDye800CW as the optimal dose, which resulted in changes in the management of 30% (3/10) of the patients [77].

Fluorescence imaging in the second NIR window is also being explored, as photon scattering suppression and

https://doi.org/10.3348/kjr.2023.0840

Korean Journal of Radiology
KJR

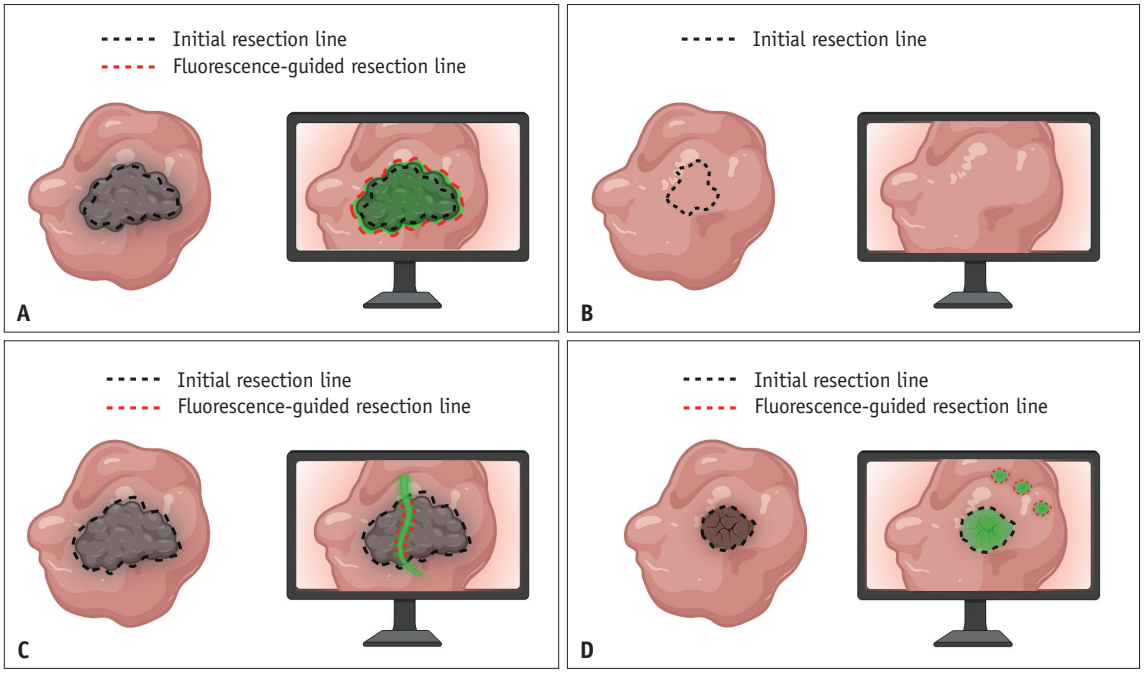

Fig. 2. Schematic diagram of the four basic applications of fluorescence-guided debulking or cytoreductive surgery. Green areas indicate fluorescence from tumors or vital structures. The gray area represents tumor tissue. **A:** Assess surgical margins. **B:** Identify clinically suspicious lesions. **C:** Protect important anatomical structures (the green area represents the fluorescence emitted by the ureter). **D:** Detect deep-tissue micrometastases.

extremely low spontaneous fluorescence in tissues compared with visible light and the NIR-I region (700–950 nm) [79] significantly improve the imaging resolution and tissue penetration depth [79]. Different biomodification strategies have also been implemented to improve the biocompatibility of inorganic nanomaterials [80] and the fluorescence properties of organic NIR-II fluorophores [81].

Most reports on fluorescence-guided surgery are confined to outcome parameters that are challenging to objectively assess and quantify, such as sensitivity, specificity, and TBR, without sufficient indication of how changes affect intraoperative decision-making, thus limiting its clinical application. A standardized clinical report should contain a pathological assessment of the consistency of the fluorescent area with the tumor and non-tumor areas, a determination of the reasonableness of additional resections, and the percentage of changes in intraoperative decision-making due to fluorescence imaging [73].

PET/MRI

PET and MRI, which provide anatomical, metabolic, and functional information, have synergistic effects and markedly improve PM diagnostic performance. PET/MRI yields a PCI closer to surgical PCI than does DWI, especially in patients with high tumor loads who do not receive chemotherapy [82]. Xi et al. [83] found that due to the extremely low liver and gastrointestinal background, ^{68}Ga-FAPI-04 PET/CT was more accurate in scoring the upper and right abdomen than ^{18}FDG PET/CT, while the left abdomen was prone to overestimation because of the stronger extension of the greater omentum and mesentery. However, the positivity rate of lower abdominal lesions was comparable to or even worse than that of ^{18}FDG PET/CT (89.19% vs. 94.59%, respectively) [83]. Further, in the small intestine, PET/MRI is more sensitive and less specific than DWI [82]. For identifying PM, PET/MRI is more effective than solely PET and MRI or in combination with CT; in 26% (5/19) of patients, PET/MRI led to a change in a clinical care plan [84]. Current evidence supports the preoperative assessment of PM by PET/MRI, which lowers radiation exposure [85]; however, it necessitates cooperation and agreement between radiologists and nuclear medicine specialists. Further research is required to ascertain the added clinical utility of PET/MRI compared to that of PET/CT and DWI/MRI.

Development of Standardized Imaging Reports

Medical imaging can also be used to select the best treatment method for peritoneal tumors. Standardized

https://doi.org/10.3348/kjr.2023.0840

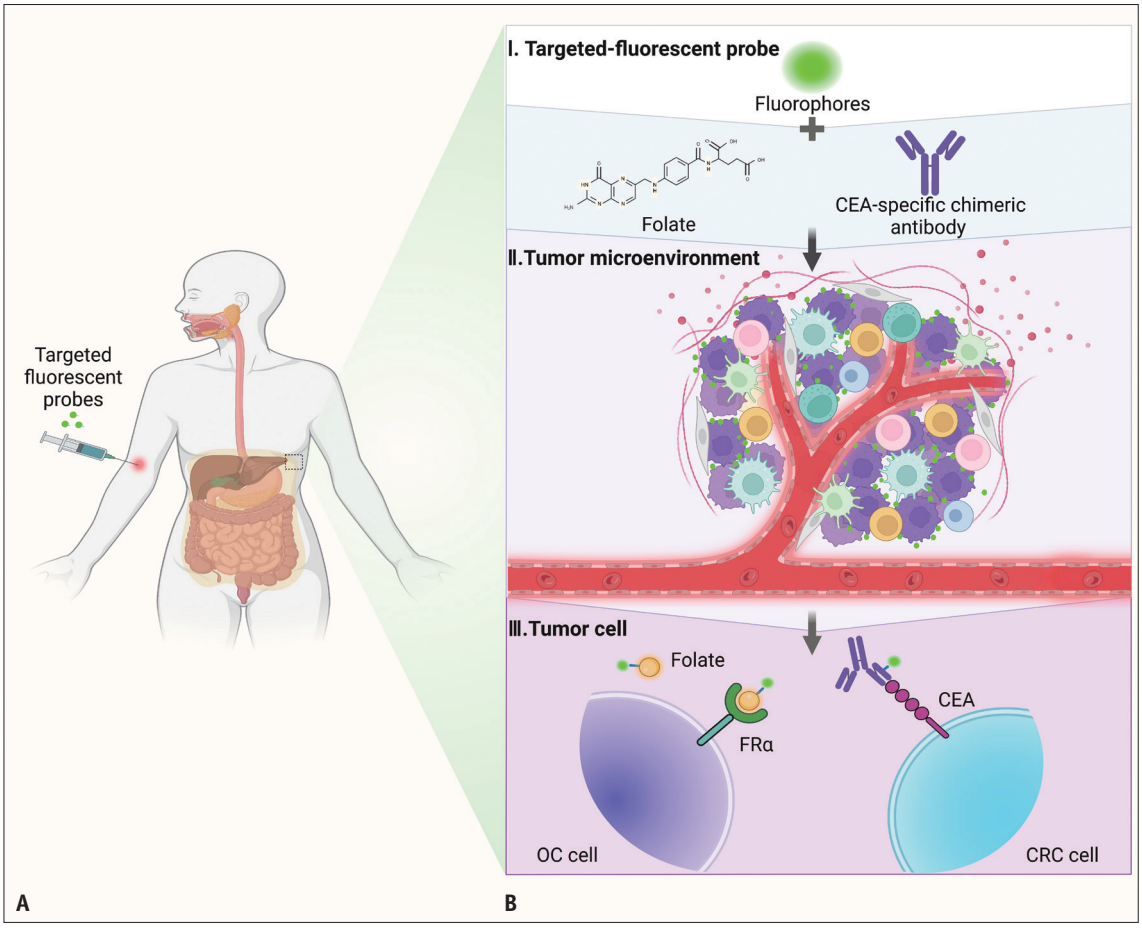

Fig. 3. Active accumulation of targeted fluorescent probes in the tumor tissue. **A:** Intravenous injection of targeted fluorescent contrast agent. **B:** Composition of targeted fluorescent tracers and two methods of targeted imaging. Near-infrared fluorescent contrast agent and targeted part (I). Active accumulation of targeted contrast agent in the tumor tissue (II). Targeting folic acid receptor in ovarian cancer and carcinoembryonic antigen in colorectal cancer (III). CEA = carcinoembryonic antigen, FRα = folate receptor alpha, OC = ovarian cancer, CRC = colorectal cancer

radiology reports should include radiological PCI findings and important imaging signs. Conventional imaging modalities underestimate actual PCI. Radiological PCI can be determined more accurately using MRI, or even a combination of CT and MRI, than using CT alone [86]. Notably, the introduction of FAPI PET/CT provides insights for surgeons to optimize surgical decision-making and detect more lesions under a high TBR. However, different regions of the abdomen may have false-positive and false-negative results, resulting in consistent imaging and surgical PCI total scores. However, the scores of these regions do not necessarily correspond to the actual tumor burden. These key imaging signs include non-resectable sites (such as diffuse small intestine and mesentery involvement), difficult-to-resect complex lesions (related to suboptimal resection), extraperitoneal metastasis (changing treatment methods), and primary cancer, all of which are closely related to the postoperative incidence and mortality, quality of life, and potential cure. The acronym PAUSE effectively summarizes the key imaging features used to determine the optimal indications for surgery and patient prognosis [87]. Table 2 summarizes the contents of PAUSE.

Radiomics and AI

Analytic Workflow

The workflow of radiomics includes image acquisition and preprocessing, tumor segmentation, feature extraction/selection, model construction, and validation (Fig. 4). Image preprocessing is primarily used to improve image quality. However, considering that different image acquisition parameters and reconstruction software may

https://doi.org/10.3348/kjr.2023.0840

Korean Journal of Radiology
KJR

Table 2. Summary of the key imaging findings of PAUSE in patients with peritoneal metastasis

	Description	Significance	Example
P: primary tumor and PCI	Quantify the degree of PM based on the size of lesions in 13 different anatomical regions of the abdomen (none, < 0.5 cm, < 5 cm, > 5 cm, corresponding to 0–3 points)	Assessment of tumor load; Cut-off values as relative indications for performing curative management	CRS: < 17 [119] GC NSRCC: < 13 SRCC: < 7 [120]
A: Ascites and abdominal wall involvement	Tumor obstruction caused by lymphatic reflux Common locations of abdominal wall diseases are port site, drain site, or in an abdominal scar	Malignant ascites usually receives palliative treatment Increase the morbidity of CRS	Malignant ascites is often palliative Lateral abdominal wall lesions are often incurable due to lymphatic drainage
U: unfavorable sites of involvement	Key anatomical sites that negatively affect surgical outcomes	Increased complexity of surgery and difficulty in achieving full CRS	Porta hepatis, hepatoduodenal ligament, falciform ligament, diaphragm, left gastric artery, portocaval space, biliary dilatation; Peri-pancreatic lesions, pyloric or duodenal obstruction; Diffuse intestinal and mesenteric involvement Hydronephrosis and ureteric involvement; Psoas, iliacus and quadratus lumborum muscle; Bladder trigone, pelvic sidewall lymph nodes and seminal vesicles
S: small bowel and mesenteric disease	Location and number of lesions involving the mesentery, and small and large bowels	Extensive infiltration and multi-segmental intestinal obstruction are not conducive to complete CRS	Bowel wall thickening/dilatation/obstruction; Mesenteric fold thickening/Mesenteric tethering; Root of mesenteric disease
E: extra peritoneal metastases	Extraperitoneal metastases involving the liver, spleen, pleura, bones, or lymph nodes	Systemic spread and advanced disease	Mostly inoperable, except for synchronous resectable liver and colorectal peritoneal metastases

PCI = peritoneal carcinomatosis index, PM = peritoneal metastasis, CRS = cytoreductive surgery, GC = gastric cancer, NSRCC = non-signet ring cell carcinoma, SRCC = signet-ring cell carcinoma

affect the performance and repeatability of the model, a universal preprocessing scheme is crucial. Tumor segmentation is affected by interobserver variability. Automated or semiautomated segmentation methods may reduce labor costs and improve the reproducibility and robustness of tumor segmentation; however, they can be affected by the complex environment of the tumor and diffuse lesions [88,89]. Furthermore, radiomics features may be unstable if extracted from small lesions, such as peritoneal seeding. Notably, relying solely on radiomics analysis of peritoneal lesions is insufficient, as the occurrence of PM depends on the synergistic effect between the primary tumor and the peritoneum [90]. Dong et al [91]. combined the radiomics signature extracted from CT images of the primary tumor and adjacent peritoneum with the Lauren classification (an independent predictor) to construct a nomogram for the preoperative prediction of occult PM in advanced GC; the area under the receiver operating characteristic curve (AUC) was 0.928. Additionally, clinical characteristics and laboratory data can be combined, often using univariate analysis, to assess their correlation with PM and improve predictive performance. The output of deep learning (DL) models can also be incorporated to improve model prediction performance.

 https://doi.org/10.3348/kjr.2023.0840

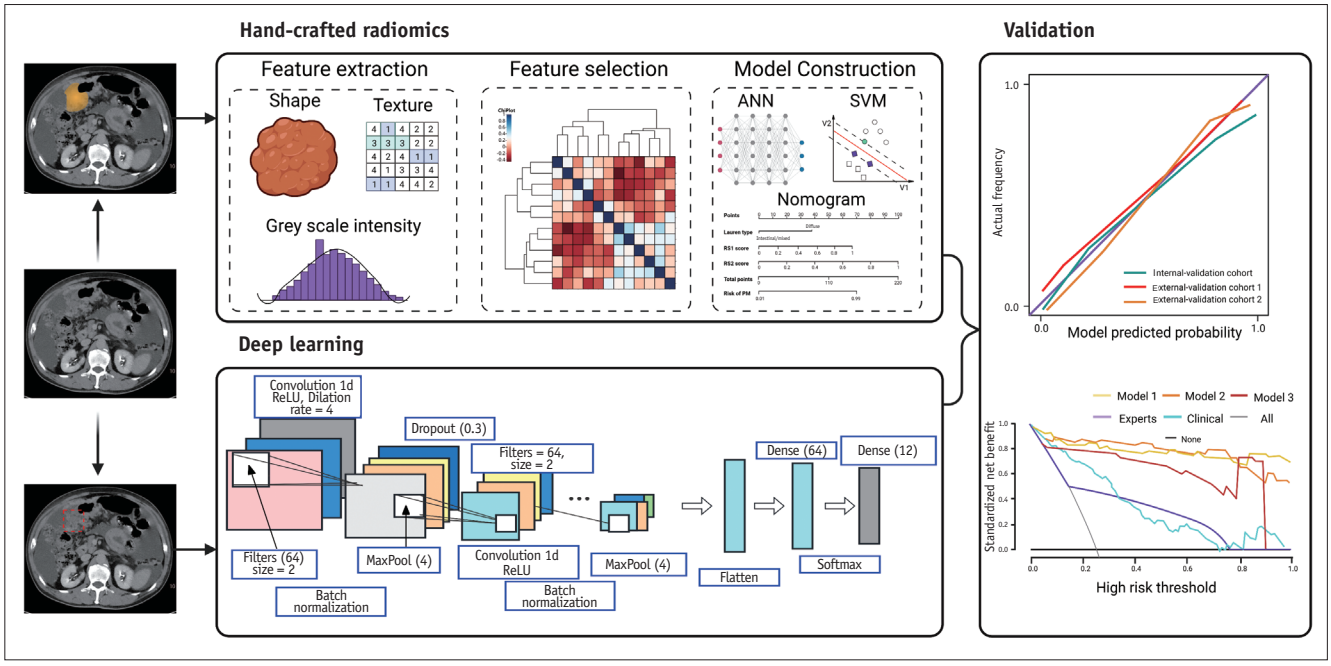

Fig. 4. Schematic diagram of the hand-crafted radiomics workflow and deep learning. The workflow of radiomics includes image acquisition and preprocessing, tumor segmentation, feature extraction/selection, model construction, and validation. For deep learning, it is an end-to-end approach with no separate feature extraction, feature selection and modelling steps. The orange area represents the depiction of tumors through manual segmentation. The red dashed square represents the use of deep learning to segment tumors. RS1 reflects the radiomics signature of the primary tumor, while RS2 reflects the radiomics signature of the peritoneum. RS1 and RS2 serve as predictive factors for PM status. ANN = Artificial Neural Network, SVM = support vector machine, ReLU = rectified linear unit, PM = peritoneal metastasis

Although the strong predictive performance of radiomics in the diagnosis of PM has been demonstrated, the interpretability and repeatability of radiomic signatures limit their clinical translation. Existing radiomics workflows lack standardization and complete methodologies, resulting in data that cannot be validated and compared for repeatability and reproducibility across multiple centers [92,93]. Medical images are often acquired using different parameters and protocols and reconstructed using different software. Consequently, institutions other than those providing data for radiomic modeling may not be able to reproduce the performance of a model or amplify it further because of potential differences in the data. Sources of variability arising from differences in multicenter CT protocols can be balanced using image compensation methods (ComBat [94]) and DL [95]. Harmonized evaluation standards and reporting guidelines are essential. Radiomics quality scoring [96] and the image biomarker standardization initiative [97] criteria for the translation of radiomics into clinically useful tests [98] are dedicated to improving study quality and establishing a standardized workflow. Therefore, each step of the imaging workflow must be carefully designed and prospectively validated using standardized assessment protocols to ensure that the workflow is coordinated and other sources of variability are reduced. Moreover, biological validation is fundamental for addressing the causal relationship between radiomic signatures and clinical outcomes, that is, discovering the biological mechanisms underlying the relationship between potential radiomic signatures and disease states. Therefore, future studies should provide the biological background of radiomic signatures, which can be analyzed using genomic data, immunohistochemistry, local pathological analysis, and habitat imaging to investigate the possible underlying mechanisms [99].

Application of Radiomics in Predicting PM

Recent studies have examined radiomics for early prediction of PM in GC, CRC, and OC (Table 3). The occurrence of PM in GC is related to both the primary site and the peritoneum; therefore, peritoneal radiomics alone are incomplete. Dong et al. [91] combined key features extracted from CT images of the primary tumor and adjacent peritoneum with the Lauren classification to construct a

https://doi.org/10.3348/kjr.2023.0840

https://doi.org/10.3348/kjr.2023.0840

Table 3. Summary of key studies on the role of radiomics in imaging of peritoneal metastasis, as applied to diagnosis, characterization, and predicting recurrence

Study	Patients, n	Imaging method	Application	ROI segmentation method	Selected radiomic features	Validation*	Best performance	Primary tumor
Dong et al. [91]	554	CT	Identify occult peritoneal metastasis	Manual	266 features	Internal (bootstrapping) External (multi-center)	AUC, 0.941 AUC, 0.928	Advanced gastric cancer
Liu et al. [100]	233	CE-CT	Preoperative prediction of occult peritoneal metastasis	Manual	539 features	Internal (split-sample)	AUC, 0.724 Accuracy, 0.575	Advanced gastric cancer
Li et al. [121]	779	CT	Preoperative prediction of peritoneal metastasis	Semi-automatic	8900	Internal (split-sample) External	AUC, 0.793 Accuracy, 0.742 AUC, 0.780 Accuracy, 0.755	Colorectal cancer
Song et al. [101]	89	Multisequence MRI	Preoperative prediction of peritoneal metastasis	Manual	1037 features	Internal (3-fold CV)	AUC, 0.944 Accuracy, 0.829	Ovarian cancer
Xue et al. [103]	355	^{18}F-FDG PET	Predicting peritoneal metastasis	Semi-automatic	69	Internal (split-sample)	AUC, 0.88	Gastric cancer
Chen et al. [122]	239	DE-CT	Predicting peritoneal metastasis	Manual	Peritoneal area, 1691 Primary tumor, 1226	Internal (split-sample)	AUC, 0.967	Gastric cancer
Yu et al. [123]	86	Multisequence MRI	Preoperative prediction of peritoneal carcinomatosis	Manual	1037	Internal	AUC, 0.902	Ovarian cancer
Masci et al. [124]	90	CT	Predicting peritoneal metastases	Manual	2 (volume and GLRLM_LRHGE)	Internal	AUC, 0.737	Gastric cancer
Li et al. [102]	141	Multisequence MRI	Predicting recurrence	Manual	1316	Internal (split-sample)	AUC, 0.78	HGSOC

*Validation methods were classified as internal (i.e., cross-validation, bootstrapping, and split-sample validation) or external validation.

ROI = region of interest, CT = computed tomography, AUC = area under the curve, CE-CT = contrast-enhanced computed tomography, MRI = magnetic resonance imaging, CV = cross-validation, FDG-PET = fluorodeoxyglucose positron emission tomography, DE-CT = dual-energy computed tomography, GLRLM_LRHGE = Grey Level Run Length Matrix_Long Run High Grey-Level Emphasis, HGSOC = high-grade serous ovarian carcinoma

Korean Journal of Radiology KJR

nomogram for the preoperative prediction of occult PM in advanced gastric cancer (AGC); the AUC was 0.928. Liu et al. [100] demonstrated that the T stage based on CT is an independent predictor of occult PM in AGC. However, most studies have used enhanced CT to extract features in the venous phase, and the effect of the delay time of different arterial phases on features requires further investigation.

The prediction model was constructed by combining the radiomic features extracted from multi-sequence MRI and the corresponding parameter maps with pelvic fluid and CA125; the AUC in the validation cohort was 0.944 [101]. A comprehensive nomogram based on preoperative multimodal MRI and clinical data to predict the peritoneal recurrence of high-grade serous ovarian carcinoma revealed an AUC of 0.78 under the validation set [102]. A limitation of these two studies is that no external validation was performed Hence, the overall performance of the method must be validated in a large multicenter study.

Radiomics in combination with ^{18}F-FDG PET has a good predictive performance for PM [103,104], but class imbalance reduces its predictive performance [105]. Xue et al. [103] combined radiomics features based on texture analysis with two predictors (CA125 and SUVmax) screened by multifactorial logistic regression analysis and showed good performance, with AUCs of 0.90 and 0.88 in the training and validation cohorts, respectively, and an accuracy of 0.75 in predicting GC PM [106]. However, an integrated model combining CT and PET radiomic features for PM of GC has not been constructed.

DL AI Models

DL can preoperatively predict PM, thereby guiding treatment decisions and avoiding unnecessary surgeries. Wei et al. [107] created DL, radiomics, and clinical models based on T2-weighted MRI images and determined the optimal weights for each branch model based on the prediction probability. Finally, they combined the three models by decision-level fusion into an integrated model that could predict PM in epithelial OC. This could be comparable to experts or even better, with AUC of 0.859 and 0.872 in the two external validation sets, respectively. Jiang et al. [108] used a DL model to predict clinically occult PM in patients with GC using preoperative CT, with an externally validated AUC of 0.920–0.946. The authors also integrated clinicopathological factors with the DL model to construct a nomogram that did not significantly improve the predictive performance, indicating that the DL model plays a dominant role in predicting occult PM. DL has also been successful in predicting response to neoadjuvant chemotherapy (NACT) in patients with OC. Yin et al. [109] developed a multi-task dynamic learning model that can simultaneously perform automatic OC segmentation and predict NACT responses and high-grade serous OC classification with a DICE of 0.78 (with values closer to one indicating better segmentation performance) and an AUC of 0.79 and 0.80, respectively, in an external validation set. Zhang et al. [110] first proposed a DL algorithm based on meta-learning to predict PM. Meta-learning can improve the generalization of the model even with limited data. However, the diagnosis of PM was not confirmed via laparoscopic exploration, and the accuracy of the findings may be obscured by false positives on enhanced CT, which is a major limitation of this study.

Peritoneal recurrence is another factor that affects the long-term survival of patients, and the key lies in the early identification of high-risk patients for peritoneal recurrence and the selection of patients who may benefit from systemic chemotherapy or local treatment (such as heated intraperitoneal chemotherapy). Jiang et al. [111] developed a DL model combining supervised contrastive learning and multi-task learning using preoperative CT images of 2320 patients to predict GC peritoneal recurrence (AUC = 0.843) and disease-free survival (0.610) in an external validation queue.

Future Perspectives and Conclusions

Accurate diagnosis of PM has significant benefits for personalized patient care, and imaging techniques for diagnosing PM have evolved rapidly over the past 20 years. The advent of numerous new imaging modalities, radiomics, and AI has driven the process of precise diagnosis from subjective, qualitative, and non-tumor-targeted to objective, quantitative, and tumor-targeted to continuously address early diagnosis, accurate evaluation, and localization of PM, further optimizing the selection of treatment methods and guiding surgeries to improve the quality of life of patients. Despite exciting advances in the technology for diagnosing PM, several challenges remain. First, although radiomics and AI have shown great potential for predicting PM and helping select appropriate surgical treatments, most studies have primarily focused on 2D images to manually outline tumor image segmentation. Given that image segmentation determines the upper limit of voxel analysis [112], whether adding 3D volume analysis and automated segmentation tools to evaluate the entire tumor will improve the

https://doi.org/10.3348/kjr.2023.0840

Korean Journal of Radiology
KJR

performance of the model requires further development and validation.

Second, although the ability of ^{68}Ga-FAPI PET/CT to diagnose more peritoneal carcinomatosis lesions can guide treatment strategies, most studies examining this phenomenon have included small sample sizes and/or diverse primary tumor types. The diagnostic value and clinical indications of ^{68}Ga-FAPI PET/CT for PM require further validation with a larger sample size from multiple centers to further investigate the sensitivity and specificity of FAPI in the tumor matrix and its advantages in TBR.

Third, PET/MRI should be a simple integration of these two technologies. Theoretically, there is a potential integration between the functional information provided by MRI and the molecular information provided by PET; only a few studies have explored this.

With the availability of numerous imaging modalities and probes, molecular imaging is no longer technically limited. Among others, the development of targeted molecular contrast agents based on nanoparticles for K-edge imaging may play an important role in the future clinical applications of SPCCT, as nanoparticles can be labeled with heavy elements and carry more targeted molecules. Designing an integrated platform for diagnosis and treatment based on the characteristics of the tumor microenvironment may change the current treatment paradigm. Two promising strategies exist. The first is to select patients with PM for FAP-targeted radionuclide therapy, as well as the quantitative and noninvasive monitoring of patients receiving such therapy, and the balance between drug efficacy and toxicity through precise adjustment of the drug dose to improve the therapeutic index. The key to achieving this is the development of FAP-targeted molecular imaging agents with high target specificity and long retention times [113]. In the second strategy, the tumor microenvironment is characterized by abnormalities, such as low pH, a disordered redox state, overexpression of enzymes, and a high concentration of glutathione, which provides precise activation of activatable fluorescent probes. Multifunctional precision diagnosis and treatment platforms (including photothermal-enhanced chemotherapy [114,115], NIR-II nanoablation [116], and multimodal NIR-II/photoacoustic (PA) therapy combined with photothermal therapy [117]) can be guided by activatable fluorescent probes for nanomedicine delivery, multimodal imaging such as PA and photothermal therapy, and photothermal therapy [118]. Therefore, the development of activatable smart NIR-II fluorescent probes with high resolution, specificity, biocompatibility, and biosafety is needed.

Future diagnostic models may combine multimodal imaging technology (anatomy, function, and metabolism) with AI-assisted diagnostic technology (radiomics combined with multiomics such as genomics, proteomics, and metabolomics) to comprehensively characterize tumor information and achieve an accurate diagnosis at different stages of PM, imaging-led therapy, and the integration of diagnosis and treatment.

Conflicts of Interest

The authors have no potential conflicts of interest to disclose.

Author Contributions

Funding acquisition: Junliang Li. Project administration: Junliang Li. Supervision: Junliang Li, Tiankang Guo, Bangxing Zhang. Writing—original draft: Chen Fu. Writing—review & editing: Junliang Li.

ORCID IDs

Chen Fu
https://orcid.org/0000-0001-8442-7500
Bangxing Zhang
https://orcid.org/0009-0006-0520-9438
Tiankang Guo
https://orcid.org/0000-0001-8556-3870
Junliang Li
https://orcid.org/0000-0002-3076-9115

Funding Statement

This research was supported by the Non-profit Central Research Institute Fund of Chinese Academy of Medical Sciences (2019PT320005, NHCDP2022028), Key Laboratory of Molecular Diagnostics and Precision Medicine for Surgical Oncology in Gansu Province (2020GSZDSYS02), the 14th Five Year Plan of Education Science of Gansu Province (GS (2021) GHB1859), Scientific Research and Innovation Fund of Gansu University of Chinese Medicine (2020KCYB-7), Longyuan Youth Innovation and Entrepreneurship Talent Project (111266548053), Teaching Research and Reform comprehensive project of Gansu University of Traditional Chinese Medicine (ZHXM-202207), and Research Fund project of Gansu Provincial Hospital (22GSSYC-1, 22GSSYB-14).

REFERENCES

1. Burg L, Timmermans M, van der Aa M, Boll D, Rovers K, de Hingh I, et al. Incidence and predictors of peritoneal metastases of gynecological origin: a population-based study in the Netherlands. *J Gynecol Oncol* 2020;31:e58
2. Thomassen I, van Gestel YR, van Ramshorst B, Luyer MD, Bosscha K, Nienhuijs SW, et al. Peritoneal carcinomatosis of gastric origin: a population-based study on incidence, survival and risk factors. *Int J Cancer* 2014;134:622-628
3. Klaver YL, Simkens LH, Lemmens VE, Koopman M, Teerenstra S, Bleichrodt RP, et al. Outcomes of colorectal cancer patients with peritoneal carcinomatosis treated with chemotherapy with and without targeted therapy. *Eur J Surg Oncol* 2012;38:617-623
4. Sadeghi B, Arvieux C, Glehen O, Beaujard AC, Rivoire M, Baulieux J, et al. Peritoneal carcinomatosis from non-gynecologic malignancies: results of the EVOCAPE 1 multicentric prospective study. *Cancer* 2000;88:358-363
5. Cortes-Guiral D, Hubner M, Alyami M, Bhatt A, Ceelen W, Glehen O, et al. Primary and metastatic peritoneal surface malignancies. *Nat Rev Dis Primers* 2021;7:91
6. Ishigami H, Fujiwara Y, Fukushima R, Nashimoto A, Yabusaki H, Imano M, et al. Phase III trial comparing intraperitoneal and intravenous paclitaxel plus S-1 versus cisplatin plus S-1 in patients with gastric cancer with peritoneal metastasis: PHOENIX-GC trial. *J Clin Oncol* 2018;36:1922-1929
7. Iwasaki Y, Terashima M, Mizusawa J, Katayama H, Nakamura K, Katai H, et al. Gastrectomy with or without neoadjuvant S-1 plus cisplatin for type 4 or large type 3 gastric cancer (JCOG0501): an open-label, phase 3, randomized controlled trial. *Gastric Cancer* 2021;24:492-502
8. Colombo N, Sessa C, du Bois A, Ledermann J, McCluggage WG, McNeish I, et al. ESMO-ESGO consensus conference recommendations on ovarian cancer: pathology and molecular biology, early and advanced stages, borderline tumours and recurrent diseasedagger. *Ann Oncol* 2019;30:672-705
9. Vergote I, Coens C, Nankivell M, Kristensen GB, Parmar MKB, Ehlen T, et al. Neoadjuvant chemotherapy versus debulking surgery in advanced tubo-ovarian cancers: pooled analysis of individual patient data from the EORTC 55971 and CHORUS trials. *Lancet Oncol* 2018;19:1680-1687
10. Yasufuku I, Nunobe S, Ida S, Kumagai K, Ohashi M, Hiki N, et al. Conversion therapy for peritoneal lavage cytology-positive type 4 and large type 3 gastric cancer patients selected as candidates for R0 resection by diagnostic staging laparoscopy. *Gastric Cancer* 2020;23:319-327
11. Solaini L, Ministrini S, Bencivenga M, D'Ignazio A, Marino E, Cipollari C, et al. Conversion gastrectomy for stage IV unresectable gastric cancer: a GIRCG retrospective cohort study. *Gastric Cancer* 2019;22:1285-1293
12. Chia DKA, Sundar R, Kim G, Ang JJ, Lum JHY, Nga ME, et al. Outcomes of a phase II study of intraperitoneal paclitaxel plus systemic capecitabine and oxaliplatin (XELOX) for gastric cancer with peritoneal metastases. *Ann Surg Oncol* 2022;29:8597-8605
13. Kepenekian V, Bhatt A, Peron J, Alyami M, Benzerdjeb N, Bakrin N, et al. Advances in the management of peritoneal malignancies. *Nat Rev Clin Oncol* 2022;19:698-718
14. Foster JM, Zhang C, Rehman S, Sharma P, Alexander HR. The contemporary management of peritoneal metastasis: a journey from the cold past of treatment futility to a warm present and a bright future. *CA Cancer J Clin* 2023;73:49-71
15. Foster JM, Sleightholm R, Patel A, Shostrom V, Hall B, Neilsen B, et al. Morbidity and mortality rates following cytoreductive surgery combined with hyperthermic intraperitoneal chemotherapy compared with other high-risk surgical oncology procedures. *JAMA Netw Open* 2019;2:e186847
16. Quenet F, Elias D, Roca L, Goere D, Ghouti L, Pocard M, et al. Cytoreductive surgery plus hyperthermic intraperitoneal chemotherapy versus cytoreductive surgery alone for colorectal peritoneal metastases (PRODIGE 7): a multicentre, randomised, open-label, phase 3 trial. *Lancet Oncol* 2021;22:256-266
17. Glehen O, Gilly FN, Boutitie F, Bereder JM, Quenet F, Sideris L, et al. Toward curative treatment of peritoneal carcinomatosis from nonovarian origin by cytoreductive surgery combined with perioperative intraperitoneal chemotherapy: a multi-institutional study of 1,290 patients. *Cancer* 2010;116:5608-5618
18. Elias D, Gilly F, Boutitie F, Quenet F, Bereder JM, Mansvelt B, et al. Peritoneal colorectal carcinomatosis treated with surgery and perioperative intraperitoneal chemotherapy: retrospective analysis of 523 patients from a multicentric French study. *J Clin Oncol* 2010;28:63-68
19. Kusamura S, Barretta F, Yonemura Y, Sugarbaker PH, Moran BJ, Levine EA, et al. The role of hyperthermic intraperitoneal chemotherapy in pseudomyxoma peritonei after cytoreductive surgery. *JAMA Surg* 2021;156:e206363
20. Jacquet P, Sugarbaker PH. Clinical research methodologies in diagnosis and staging of patients with peritoneal carcinomatosis. *Cancer Treat Res* 1996;82:359-374
21. Elzarkaa AA, Shaalan W, Elemam D, Mansour H, Melis M, Malik E, et al. Peritoneal cancer index as a predictor of survival in advanced stage serous epithelial ovarian cancer: a prospective study. *J Gynecol Oncol* 2018;29:e47
22. Li J, Guo T. Role of peritoneal mesothelial cells in the progression of peritoneal metastases. *Cancers (Basel)* 2022;14:2856
23. van 't Sant I, Engbersen MP, Bhairosing PA, Lambregts DMJ, Beets-Tan RGH, van Driel WJ, et al. Diagnostic performance of imaging for the detection of peritoneal metastases: a meta-analysis. *Eur Radiol* 2020;30:3101-3112
24. Chang-Yun L, Yonemura Y, Ishibashi H, Sako S, Tsukiyama G, Kitai T, et al. Evaluation of preoperative computed tomography in estimating peritoneal cancer index in peritoneal carcinomatosis. *Gan To Kagaku Ryoho* 2011;38:2060-2064
25. de Bree E, Koops W, Kroger R, van Ruth S, Witkamp AJ,

https://doi.org/10.3348/kjr.2023.0840

Zoetmulder FA. Peritoneal carcinomatosis from colorectal or appendiceal origin: correlation of preoperative CT with intraoperative findings and evaluation of interobserver agreement. *J Surg Oncol* 2004;86:64-73
26. Chia CS, Wong LCK, Hennedige TP, Ong WS, Zhu HY, Tan GHC, et al. Prospective comparison of the performance of mri versus CT in the detection and evaluation of peritoneal surface malignancies. *Cancers (Basel)* 2022;14:3179
27. An H, Perucho JAU, Chiu KWH, Hui ES, Chu MMY, Ngu SF, et al. Association between high diffusion-weighted imaging-derived functional tumor burden of peritoneal carcinomatosis and overall survival in patients with advanced ovarian carcinoma. *Korean J Radiol* 2022;23:539-547
28. Bonnin A, Durot C, Djelouah M, Dohan A, Arrivé L, Rousset P, et al. MR imaging of the perihepatic space. *Korean J Radiol* 2021;22:547-558
29. Govaerts K, Lurvink RJ, De Hingh I, Van der Speeten K, Villeneuve L, Kusamura S, et al. Appendiceal tumours and pseudomyxoma peritonei: Literature review with PSOGI/EURACAN clinical practice guidelines for diagnosis and treatment. *Eur J Surg Oncol* 2021;47:11-35
30. Delhorme JB, Villeneuve L, Bouche O, Averous G, Dohan A, Gornet JM, et al. Appendiceal tumors and pseudomyxoma peritonei: french intergroup clinical practice guidelines for diagnosis, treatments and follow-up (RENAPE, RENAPATH, SNFGE, FFCD, GERCOR, UNICANCER, SFCD, SFED, SFRO, ACHBT, SFR). *Dig Liver Dis* 2022;54:30-39
31. Dhanda S, Thakur M, Kerkar R, Jagmohan P. Diffusion-weighted imaging of gynecologic tumors: diagnostic pearls and potential pitfalls. *Radiographics* 2014;34:1393-1416
32. Padhani AR, Liu G, Koh DM, Chenevert TL, Thoeny HC, Takahara T, et al. Diffusion-weighted magnetic resonance imaging as a cancer biomarker: consensus and recommendations. *Neoplasia* 2009;11:102-125
33. Panagiotidis E, Datseris IE, Exarhos D, Skilakaki M, Skoura E, Bamias A. High incidence of peritoneal implants in recurrence of intra-abdominal cancer revealed by 18F-FDG PET/CT in patients with increased tumor markers and negative findings on conventional imaging. *Nucl Med Commun* 2012;33:431-438
34. Saiz Martínez R, Dromain C, Vietti Violi N. Imaging of gastric carcinomatosis. *J Clin Med* 2021;10:5294
35. Delgado Bolton RC, Aide N, Colletti PM, Ferrero A, Paez D, Skanjeti A, et al. EANM guideline on the role of 2-[18F] FDG PET/CT in diagnosis, staging, prognostic value, therapy assessment and restaging of ovarian cancer, endorsed by the american college of nuclear medicine (ACNM), the society of nuclear medicine and molecular imaging (SNMMI) and the International atomic energy agency (IAEA). *Eur J Nucl Med Mol Imaging* 2021;48:3286-3302
36. Yu X, Lee EYP, Lai V, Chan Q. Correlation between tissue metabolism and cellularity assessed by standardized uptake value and apparent diffusion coefficient in peritoneal metastasis. *J Magn Reson Imaging* 2014;40:99-105
37. Soyka JD, Strobel K, Veit-Haibach P, Schaefer NG, Schmid DT, Tschopp A, et al. Influence of bowel preparation before 18F-FDG PET/CT on physiologic 18F-FDG activity in the intestine. *J Nucl Med* 2010;51:507-510
38. Honma Y, Terauchi T, Tateishi U, Kano D, Nagashima K, Shoji H, et al. Imaging peritoneal metastasis of gastric cancer with (18)F-fluorothymidine positron emission tomography/computed tomography: a proof-of-concept study. *Br J Radiol* 2018;91:20180259
39. Akin EA, Qazi ZN, Osman M, Zeman RK. Clinical impact of FDG PET/CT in alimentary tract malignancies: an updated review. *Abdom Radiol (NY)* 2020;45:1018-1035
40. Lin R, Lin Z, Chen Z, Zheng S, Zhang J, Zang J, et al. [(68)Ga] Ga-DOTA-FAPI-04 PET/CT in the evaluation of gastric cancer: comparison with [(18)F]FDG PET/CT. *Eur J Nucl Med Mol Imaging* 2022;49:2960-2971
41. Yousefi M, Dehghani S, Nosrati R, Ghanei M, Salmaninejad A, Rajaie S, et al. Current insights into the metastasis of epithelial ovarian cancer - hopes and hurdles. *Cell Oncol (Dordr)* 2020;43:515-538
42. Willemink MJ, Persson M, Pourmorteza A, Pelc NJ, Fleischmann D. Photon-counting CT: technical principles and clinical prospects. *Radiology* 2018;289:293-312
43. Greffier J, Villani N, Defez D, Dabli D, Si-Mohamed S. Spectral CT imaging: technical principles of dual-energy CT and multi-energy photon-counting CT. *Diagn Interv Imaging* 2023;104:167-177
44. Rajendran K, Petersilka M, Henning A, Shanblatt ER, Schmidt B, Flohr TG, et al. First clinical photon-counting detector CT system: technical evaluation. *Radiology* 2022;303:130-138
45. Esquivel A, Ferrero A, Mileto A, Baffour F, Horst K, Rajiah PS, et al. Photon-counting detector CT: key points radiologists should know. *Korean J Radiol* 2022;23:854-865
46. Decker JA, Bette S, Lubina N, Rippel K, Braun F, Risch F, et al. Low-dose CT of the abdomen: Initial experience on a novel photon-counting detector CT and comparison with energy-integrating detector CT. *Eur J Radiol* 2022;148:110181
47. Thivolet A, Si-Mohamed S, Bonnot P-E, Blanchet C, Képénékian V, Boussel L, et al. Spectral photon-counting CT imaging of colorectal peritoneal metastases: initial experience in rats. *Sci Rep* 2020;10:13394
48. Sartoretti T, Landsmann A, Nakhostin D, Eberhard M, Roeren C, Mergen V, et al. Quantum iterative reconstruction for abdominal photon-counting detector CT improves image quality. *Radiology* 2022;303:339-348
49. Mona CE, Benz MR, Hikmat F, Grogan TR, Lueckerath K, Razmaria A, et al. Correlation of 68Ga-FAPi-46 PET biodistribution with FAP expression by immunohistochemistry in patients with solid cancers: interim analysis of a prospective translational exploratory study. *J Nucl Med* 2022;63:1021-1026
50. Gilardi L, Airò Farulla LS, Demirci E, Clerici I, Omodeo Salè E, Ceci F. Imaging Cancer-Associated Fibroblasts (CAFs) with FAPi PET. *Biomedicines* 2022;10:523

 https://doi.org/10.3348/kjr.2023.0840

51. Fitzgerald AA, Weiner LM. The role of fibroblast activation protein in health and malignancy. *Cancer Metastasis Reviews* 2020;39:783-803
52. Koerber SA, Staudinger F, Kratochwil C, Adeberg S, Haefner MF, Ungerechts G, et al. The role of 68Ga-FAPI PET/CT for patients with malignancies of the lower gastrointestinal tract: first clinical experience. *J Nucl Med* 2020;61:1331-1336
53. Altmann A, Haberkorn U, Siveke J. The latest developments in imaging of fibroblast activation protein. *J Nucl Med* 2021;62:160-167
54. Wang S, Zhou X, Xu X, Ding J, Liu S, Hou X, et al. Clinical translational evaluation of Al18F-NOTA-FAPI for fibroblast activation protein-targeted tumour imaging. *Eur J Nucl Med Mol Imaging* 2021;48:4259-4271
55. Sahnoun S, Conen P, Mottaghy FM. The battle on time, money and precision: Da[18F] id vs. [68Ga]liath. *Eur J Nucl Med Mol Imaging* 2020;47:2944-2946
56. Hu K, Wang L, Wu H, Huang S, Tian Y, Wang Q, et al. [(18)F] FAPI-42 PET imaging in cancer patients: optimal acquisition time, biodistribution, and comparison with [(68)Ga]Ga-FAPI-04. *Eur J Nucl Med Mol Imaging* 2022;49:2833-2843
57. Lindner T, Loktev A, Altmann A, Giesel F, Kratochwil C, Debus J, et al. Development of quinoline-based theranostic ligands for the targeting of fibroblast activation protein. *J Nucl Med* 2018;59:1415-1422
58. Loktev A, Lindner T, Mier W, Debus J, Altmann A, Jager D, et al. A tumor-imaging method targeting cancer-associated fibroblasts. *J Nucl Med* 2018;59:1423-1429
59. Watabe T, Liu Y, Kaneda-Nakashima K, Shirakami Y, Lindner T, Ooe K, et al. Theranostics targeting fibroblast activation protein in the tumor stroma: (64)Cu- and (225)Ac-Labeled FAPI-04 in pancreatic cancer xenograft mouse models. *J Nucl Med* 2020;61:563-569
60. Prashanth A, Kumar Ravichander S, Eswaran P, Kalyan S, Maheswari Babu S. Diagnostic performance of Ga-68 FAPI 04 PET/CT in colorectal malignancies. *Nucl Med Commun* 2023;44:276-283
61. Güzel Y, Kaplan İ. Comparison of (68)GA-FAPI-04 PET/CT and (18)F-FDG PET/CT findings in peritonitis carcinomatosa cases. *Hell J Nucl Med* 2023;26:26-34
62. Zhao L, Pang Y, Luo Z, Fu K, Yang T, Zhao L, et al. Role of [68Ga]Ga-DOTA-FAPI-04 PET/CT in the evaluation of peritoneal carcinomatosis and comparison with [18F]-FDG PET/CT. *Eur J Nucl Med Mol Imaging* 2021;48:1944-1955
63. Chen H, Zhao L, Ruan D, Pang Y, Hao B, Dai Y, et al. Usefulness of [(68)Ga]Ga-DOTA-FAPI-04 PET/CT in patients presenting with inconclusive [(18)F]FDG PET/CT findings. *Eur J Nucl Med Mol Imaging* 2021;48:73-86
64. Capobianco A, Cottone L, Monno A, Manfredi AA, Rovere-Querini P. The peritoneum: healing, immunity, and diseases. *J Pathol* 2017;243:137-147
65. Mori Y, Dendl K, Cardinale J, Kratochwil C, Giesel FL, Haberkorn U. FAPI PET: fibroblast activation protein inhibitor use in oncologic and nononcologic disease. *Radiology* 2023;306:e220749
66. Calais J, Mona CE. Will FAPI PET/CT Replace FDG PET/CT in the next decade? point-an important diagnostic, phenotypic, and biomarker role. *AJR Am J Roentgenol* 2021;216:305-306
67. Li C, Tian Y, Chen J, Jiang Y, Xue Z, Xing D, et al. Usefulness of [68Ga]FAPI-04 and [18F]FDG PET/CT for the detection of primary tumour and metastatic lesions in gastrointestinal carcinoma: a comparative study. *Eur Radiol* 2023;33:2779-2791
68. Liu S, Feng Z, Xu X, Ge H, Ju X, Wu X, et al. Head-to-head comparison of [(18)F]-FDG and [(68) Ga]-DOTA-FAPI-04 PET/CT for radiological evaluation of platinum-sensitive recurrent ovarian cancer. *Eur J Nucl Med Mol Imaging* 2023;50:1521-1531
69. Elboga U, Sahin E, Kus T, Cayirli YB, Aktas G, Okuyan M, et al. Comparison of 68Ga-FAPI PET/CT and 18FDG PET/CT modalities in gastrointestinal system malignancies with peritoneal involvement. *Mol Imaging Biol* 2022;24:789-797
70. Pang Y, Zhao L, Luo Z, Hao B, Wu H, Lin Q, et al. Comparison of (68)Ga-FAPI and (18)F-FDG uptake in gastric, duodenal, and colorectal cancers. *Radiology* 2021;298:393-402
71. Gege Z, Xueju W, Bin J. Head-to-head comparison of 68Ga-FAPI PET/CT and FDG PET/CT for the detection of peritoneal metastases: systematic review and meta-analysis. *AJR Am J Roentgenol* 2023;220:490-498
72. Waumans Y, Baerts L, Kehoe K, Lambeir AM, De Meester I. The dipeptidyl peptidase family, prolyl oligopeptidase, and prolyl carboxypeptidase in the immune system and inflammatory disease, including atherosclerosis. *Front Immunol* 2015;6:387
73. Lauwerends LJ, van Driel P, Baatenburg de Jong RJ, Hardillo JAU, Koljenovic S, Puppels G, et al. Real-time fluorescence imaging in intraoperative decision making for cancer surgery. *Lancet Oncol* 2021;22:e186-e195
74. Tanyi JL, Randall LM, Chambers SK, Butler KA, Winer IS, Langstraat CL, et al. A Phase III study of pafolacianine injection (OTL38) for Intraoperative Imaging of folate receptor-positive ovarian cancer (study 006). *J Clin Oncol* 2023;41:276-284
75. Randall LM, Wenham RM, Low PS, Dowdy SC, Tanyi JL. A phase II, multicenter, open-label trial of OTL38 injection for the intra-operative imaging of folate receptor-alpha positive ovarian cancer. *Gynecol Oncol* 2019;155:63-68
76. Shen J, Hu Y, Putt KS, Singhal S, Han H, Visscher DW, et al. Assessment of folate receptor alpha and beta expression in selection of lung and pancreatic cancer patients for receptor targeted therapies. *Oncotarget* 2017;9:4485-4495
77. de Gooyer JM, Elekonawo FMK, Bremers AJA, Boerman OC, Aarntzen E, de Reuver PR, et al. Multimodal CEA-targeted fluorescence and radioguided cytoreductive surgery for peritoneal metastases of colorectal origin. *Nat Commun* 2022;13:2621
78. Schaap DP, de Valk KS, Deken MM, Meijer RPJ, Burggraaf J, Vahrmeijer AL, et al. Carcinoembryonic antigen-specific, fluorescent image-guided cytoreductive surgery with

hyperthermic intraperitoneal chemotherapy for metastatic colorectal cancer. *Br J Surg* 2020;107:334-337
79. Yang RQ, Lou KL, Wang PY, Gao YY, Zhang YQ, Chen M, et al. Surgical navigation for malignancies guided by near-infrared-II fluorescence imaging. *Small Methods* 2021;5:e2001066
80. Wang P, Li J, Wei M, Yang R, Lou K, Dang Y, et al. Tumor-microenvironment triggered signal-to-noise boosting nanoprobes for NIR-IIb fluorescence imaging guided tumor surgery and NIR-II photothermal therapy. *Biomaterials* 2022;287:121636
81. Meng X, Pang X, Zhang K, Gong C, Yang J, Dong H, et al. Recent advances in near-infrared-II fluorescence imaging for deep-tissue molecular analysis and cancer diagnosis. *Small* 2022;18:e2202035
82. Jónsdóttir B, Ripoll MA, Bergman A, Silins I, Poromaa IS, Ahlström H, et al. Validation of (18)F-FDG PET/MRI and diffusion-weighted MRI for estimating the extent of peritoneal carcinomatosis in ovarian and endometrial cancer -a pilot study. *Cancer Imaging* 2021;21:34
83. Xi Y, Sun L, Che X, Huang X, Liu H, Wang Q, et al. A comparative study of [68Ga]Ga-FAPI-04 PET/MR and [18F]FDG PET/CT in the diagnostic accuracy and resectability prediction of ovarian cancer. *Eur J Nucl Med Mol Imaging* 2023;50:2885-2898
84. Furtado FS, Wu MZ, Esfahani SA, Ferrone CR, Blaszkowsky LS, Clark JW, et al. Positron emission tomography/magnetic resonance imaging (PET/MRI) versus the standard of care imaging in the diagnosis of peritoneal carcinomatosis. *Ann Surg* 2023;277:e893-e899
85. Sawicki LM, Kirchner J, Grueneisen J, Ruhlmann V, Aktas B, Schaarschmidt BM, et al. Comparison of (18)F-FDG PET/MRI and MRI alone for whole-body staging and potential impact on therapeutic management of women with suspected recurrent pelvic cancer: a follow-up study. *Eur J Nucl Med Mol Imaging* 2018;45:622-629
86. Dohan A, Hoeffel C, Soyer P, Jannot AS, Valette PJ, Thivolet A, et al. Evaluation of the peritoneal carcinomatosis index with CT and MRI. *Br J Surg* 2017;104:1244-1249
87. Chandramohan A, Thrower A, Smith SA, Shah N, Moran B. "PAUSE": a method for communicating radiological extent of peritoneal malignancy. *Clin Radiol* 2017;72:972-980
88. Choi Y, Nam Y, Lee YS, Kim J, Ahn KJ, Jang J, et al. IDH1 mutation prediction using MR-based radiomics in glioblastoma: comparison between manual and fully automated deep learning-based approach of tumor segmentation. *Eur J Radiol* 2020;128:109031
89. de Sitter A, Verhoeven T, Burggraaff J, Liu Y, Simoes J, Ruggieri S, et al. Reduced accuracy of MRI deep grey matter segmentation in multiple sclerosis: an evaluation of four automated methods against manual reference segmentations in a multi-center cohort. *J Neurol* 2020;267:3541-3554
90. Fidler IJ. The pathogenesis of cancer metastasis: the 'seed and soil' hypothesis revisited. *Nat Rev Cancer* 2003;3:453-458
91. Dong D, Tang L, Li ZY, Fang MJ, Gao JB, Shan XH, et al. Development and validation of an individualized nomogram to identify occult peritoneal metastasis in patients with advanced gastric cancer. *Ann Oncol* 2019;30:431-438
92. Hatt M, Tixier F, Pierce L, Kinahan PE, Le Rest CC, Visvikis D. Characterization of PET/CT images using texture analysis: the past, the present... any future? *Eur J Nucl Med Mol Imaging* 2017;44:151-165
93. Foy JJ, Robinson KR, Li H, Giger ML, Al-Hallaq H, Armato SG, 3rd. Variation in algorithm implementation across radiomics software. *J Med Imaging (Bellingham)* 2018;5:044505
94. Orlhac F, Frouin F, Nioche C, Ayache N, Buvat I. Validation of a method to compensate multicenter effects affecting ct radiomics. *Radiology* 2019;291:53-59
95. Lee SB, Cho YJ, Hong Y, Jeong D, Lee J, Kim SH, et al. Deep learning-based image conversion improves the reproducibility of computed tomography radiomics features: a phantom study. *Invest Radiol* 2022;57:308-317
96. Radiomics quality score - RQS 2.0 (under development) [accessed on September 28, 2023]. Available at: https://www.radiomics.world/rqs2
97. Zwanenburg A, Vallieres M, Abdalah MA, Aerts H, Andrearczyk V, Apte A, et al. The image biomarker standardization initiative: standardized quantitative radiomics for high-throughput image-based phenotyping. *Radiology* 2020;295:328-338
98. Huang EP, O'Connor JPB, McShane LM, Giger ML, Lambin P, Kinahan PE, et al. Criteria for the translation of radiomics into clinically useful tests. *Nat Rev Clin Oncol* 2023;20:69-82
99. Tomaszewski MR, Gillies RJ. The biological meaning of radiomic features. *Radiology* 2021;298:505-516
100. Liu S, He J, Liu S, Ji C, Guan W, Chen L, et al. Radiomics analysis using contrast-enhanced CT for preoperative prediction of occult peritoneal metastasis in advanced gastric cancer. *Eur Radiol* 2020;30:239-246
101. Song XL, Ren JL, Yao TY, Zhao D, Niu J. Radiomics based on multisequence magnetic resonance imaging for the preoperative prediction of peritoneal metastasis in ovarian cancer. *Eur Radiol* 2021;31:8438-8446
102. Li C, Wang H, Chen Y, Fang M, Zhu C, Gao Y, et al. A nomogram combining MRI multisequence radiomics and clinical factors for predicting recurrence of high-grade serous ovarian carcinoma. *J Oncol* 2022;2022:1716268
103. Xue B, Jiang J, Chen L, Wu S, Zheng X, Zheng X, et al. Development and validation of a radiomics model based on (18)F-FDG PET of primary gastric cancer for predicting peritoneal metastasis. *Front Oncol* 2021;11:740111
104. Liu Q, Li J, Xin B, Sun Y, Feng D, Fulham MJ, et al. (18) F-FDG PET/CT radiomics for preoperative prediction of lymph node metastases and nodal staging in gastric cancer. *Front Oncol* 2021;11:723345
105. Pullen LCE, Noortman WA, Triemstra L, de Jongh C, Rademaker FJ, Spijkerman R, et al. Prognostic value of [18F]FDG PET radiomics to detect peritoneal and distant metastases in locally advanced gastric cancer--a side study of the

prospective multicentre PLASTIC study. *Cancers (Basel)* 2023;15:2874
106. Huang W, Zhou K, Jiang Y, Chen C, Yuan Q, Han Z, et al. Radiomics nomogram for prediction of peritoneal metastasis in patients with gastric cancer. *Front Oncol* 2020;10:1416
107. Wei M, Zhang Y, Ding C, Jia J, Xu H, Dai Y, et al. Associating peritoneal metastasis with T2-weighted MRI images in epithelial ovarian cancer using deep learning and radiomics: a multicenter study. *J Magn Reson Imaging* 2023 May 3. [Epub]. https://doi.org/10.1002/jmri.28761
108. Jiang Y, Liang X, Wang W, Chen C, Yuan Q, Zhang X, et al. Noninvasive prediction of occult peritoneal metastasis in gastric cancer using deep learning. *JAMA Netw Open* 2021;4:e2032269
109. Yin R, Guo Y, Wang Y, Zhang Q, Dou Z, Wang Y, et al. Predicting neoadjuvant chemotherapy response and high-grade serous ovarian cancer from CT images in ovarian cancer with multitask deep learning: a multicenter study. *Acad Radiol* 2023;30 Suppl 2:S192-S201
110. Zhang H, Zhu X, Li B, Dai X, Bao X, Fu Q, et al. Development and validation of a meta-learning-based multi-modal deep learning algorithm for detection of peritoneal metastasis. *Int J Comput Assist Radiol Surg* 2022;17:1845-1853
111. Jiang Y, Zhang Z, Yuan Q, Wang W, Wang H, Li T, et al. Predicting peritoneal recurrence and disease-free survival from CT images in gastric cancer with multitask deep learning: a retrospective study. *Lancet Digit Health* 2022;4:e340-e350
112. Balagurunathan Y, Gu Y, Wang H, Kumar V, Grove O, Hawkins S, et al. Reproducibility and prognosis of quantitative features extracted from CT images. *Transl Oncol* 2014;7:72-87
113. Zhao L, Niu B, Fang J, Pang Y, Li S, Xie C, et al. Synthesis, preclinical evaluation, and a pilot clinical PET imaging study of (68)Ga-labeled FAPI dimer. *J Nucl Med* 2022;63:862-868
114. Sun T, Zhang G, Ning T, Chen Q, Chu Y, Luo Y, et al. A versatile theranostic platform for colorectal cancer peritoneal metastases: real-time tumor-tracking and photothermal-enhanced chemotherapy. *Adv Sci (Weinh)* 2021;8:e2102256
115. Li H, Liu Y, Huang B, Zhang C, Wang Z, She W, et al. Highly efficient GSH-responsive "off-on" NIR-II fluorescent fenton nanocatalyst for multimodal imaging-guided photothermal/chemodynamic synergistic cancer therapy. *Anal Chem* 2022;94:10470-10478
116. Ling S, Yang X, Li C, Zhang Y, Yang H, Chen G, et al. Tumor microenvironment-activated NIR-II nanotheranostic system for precise diagnosis and treatment of peritoneal metastasis. *Angew Chem Int Ed Engl* 2020;59:7219-7223
117. Zhang R, Xu Y, Zhang Y, Kim HS, Sharma A, Gao J, et al. Rational design of a multifunctional molecular dye for dual-modal NIR-II/photoacoustic imaging and photothermal therapy. *Chem Sci* 2019;10:8348-8353
118. Zhang Z, Xu W, Kang M, Wen H, Guo H, Zhang P, et al. An all-round athlete on the track of phototheranostics: subtly regulating the balance between radiative and nonradiative decays for multimodal imaging-guided synergistic therapy. *Adv Mater* 2020;32:e2003210
119. Goere D, Souadka A, Faron M, Cloutier AS, Viana B, Honore C, et al. Extent of colorectal peritoneal carcinomatosis: attempt to define a threshold above which HIPEC does not offer survival benefit: a comparative study. *Ann Surg Oncol* 2015;22:2958-2964
120. Bonnot PE, Lintis A, Mercier F, Benzerdjeb N, Passot G, Pocard M, et al. Prognosis of poorly cohesive gastric cancer after complete cytoreductive surgery with or without hyperthermic intraperitoneal chemotherapy (CYTO-CHIP study). *Br J Surg* 2021;108:1225-1235
121. Li M, Sun K, Dai W, Xiang W, Zhang Z, Zhang R, et al. Preoperative prediction of peritoneal metastasis in colorectal cancer using a clinical-radiomics model. *Eur J Radiol* 2020;132:109326
122. Chen Y, Xi W, Yao W, Wang L, Xu Z, Wels M, et al. Dual-energy computed tomography-based radiomics to predict peritoneal metastasis in gastric cancer. *Front Oncol* 2021;11:659981
123. Yu XY, Ren J, Jia Y, Wu H, Niu G, Liu A, et al. Multiparameter MRI radiomics model predicts preoperative peritoneal carcinomatosis in ovarian cancer. *Front Oncol* 2021;11:765652
124. Masci GM, Ciccarelli F, Mattei FI, Grasso D, Accarpio F, Catalano C, et al. Role of CT texture analysis for predicting peritoneal metastases in patients with gastric cancer. *Radiol Med* 2022;127:251-258